

# A Detailed Benchmark and Modeling of the Excited and Emissive States of A Salen Type Tetradentate Schiff Base and Its Zn(II) Complex: Synthesis, Characterization, Fluorescence and TD-DFT Study

Bir Salen Tipi Schiff Bazı ve Zn(II) Kompleksinin Uyarılmış ve Emisif Hallerinin Ayrıntılı Bir Kıyaslaması ve Modellenmesi: Sentez, Karakterizasyon, Floresans ve TD-DFT Çalışması

Research Article

**Serkan Demir**

Department of Industrial Engineering, Faculty of Engineering, Giresun University, Giresun, Turkey.

## ABSTRACT

A 2:1 condensation of 2-hydroxy naphthaldehyde with 1,3-diaminopropane have resulted symmetrical tetradentate NNOO Schiff base ligand namely N,N -bis(2-hydroxy-naphthaldimine)-2,3-diaminopropane (napdap) and 1:1 mixing of this ligand with  $Zn(ClO_4)_2 \cdot 6H_2O$  in THF yielded the complex (N,N -bis(2-hydroxy-naphthaldimine)-2,3-diaminopropanato)zinc(II) (1). Characterizations of the compounds have been carried out by Elemental analyses, IR spectroscopy, Electro-spray ionization mass spectroscopy (ESI-MS), Thermal analysis and conductivity measurements. Excited state and emission profiles of the compounds have been investigated by UV-Vis absorbtion spectroscopy and steady state fluorescence spectroscopy techniques. Vertical excitations of the compounds responsible for their emissions have been further probed by ab-initio time dependent-density functional theory (TD-DFT) studies.

## Key Words

Fluorescence spectroscopy, tetradentate Schiff base, TD-DFT, ESI-mass spectroscopy, salen-Zn(II) complex.

## Öz

2-hidroksinaftaldehit ve 1,3-diaminopropanın 2:1 kondenzasyonu sonucu simetrik dört dişli NNOO Schiff bazı ligantı, N,N -bis(2-hidroksi-naftaldimin)-2,3-diaminopropan (napdap) ve ligantın  $Zn(ClO_4)_2 \cdot 6H_2O$  ile THF içerisinde 1:1 karıştırılması ile (N,N -bis(2-hidroksi-naftaldimin)-2,3-diaminopropanato)çinko(II) kompleksi (1) sentezlendi. Bileşiklerin karakterizasyonları Elementel analiz, IR spektroskopisi, Elektro-sprey iyonlaşma kütle spektroskopisi (ESI-MS), Termik analiz and iletkenlik ölçümleri ile yapıldı. Bileşiklerin uyarılmış hal ve emisif özellikleri UV-Vis absorpsiyon spektroskopisi ve kararlı hal floresans spektroskopisi teknikleri ile incelendi. Bileşiklerin emisyonlarından sorumlu dikey uyarılma geçişleri daha ayrıntılı olarak ab-initio zamana-bağlı yoğunluk fonksiyonel teorisi çalışmaları ile incelendi.

## Anahtar Kelimeler

Floresans spektroskopisi, dört-dişli Schiff bazı, TD-DFT, ESI-kütle spektroskopisi, salen-Zn(II) kompleksi.

**Article History:** Received: Mar 9, 2016; Revised: Jun 9, 2016; Accepted: Oct 20, 2016; Available Online: Dec 31, 2016.

**DOI:** 10.15671/HJBC.2016.126

**Correspondence to:** S. Demir, Department of Industrial Engineering, Faculty of Engineering, Giresun University, Giresun, Turkey.

Tel: +90 531 791 7029

Fax: +90 454 1749

E-Mail: serkan.demir@giresun.edu.tr

## INTRODUCTION

The coordination chemistry of zinc as the second most abundant trace metal after iron in human or other mammals [1] has become a rapid growing research area particularly with biological aspects of the metal. As a result of its flexible coordination geometry, fast ligand exchange, Lewis acidity, intermediate polarizability, strong binding to suitable sites, and its redox inactivity within biological environments [2], zinc plays diverse functional roles in many life-sustaining biochemical processes including catalytic active center of over 300 zinc containing enzymes, structural co-factors, regulator of enzymes, gene expression, DNA binding, neuronal signal transmission, and key structural components of a huge number of enzyme or non-enzyme proteins [3-10]. Other than these tightly bound type of zinc, the existence of loosely bound mobile or chelatable zinc has been also identified in diverse locations in human body including brain, prostate, intestine, pancreas, and spermatozoa [11-15]. Chelatable zinc takes part in many pathological processes such as apoptosis, neuronal injury in certain acute conditions, epilepsy, cerebral ischemia, infantile diarrhea, and Alzheimer's disease [16-23].

Studies based on tightly bound type of zinc focus mostly on mimetics of the active sites of biologically relevant enzymes such as carbonic anhydrase, carboxy peptidase and liver alcohol dehydrogenase [24] and these based on loosely bound zinc are mainly consist of spectroscopic biosensing of the metal. Among the methods to detect chelatable zinc, the most powerful one is fluorescence spectroscopy [25]. Because of closed-shell  $d^{10}$  electronic configuration and the absence of redox activity of the metal in biological environments, common techniques like UV-Vis, Mössbauer, NMR, EPR spectroscopy, and magnetic measurements are ineffective whereas zinc(II) changes the fluorescence intensity of organic fluorophore either by enhancement or with quenching and thus, fluorescence spectroscopy of the zinc (II) complexes can be studied effectively. Despite the fact that many reports demonstrated the significance of chelatable zinc in biological environments, the action mechanisms of the metal are relatively less

known than those of other cations like  $Ca^{2+}$ ,  $Na^+$ , and  $K^+$  [26]. Therefore, there is a renewed and remarkable interest of research for chelatable zinc in biological environments [27-29].

Schiff base metal complexes are excessively studied due to their wide applications. Among these large classes of compounds, metal complexes of salen (N,N -bis(salicylidene) ethylenediamine) or salophen (N,N -bis(salicylidene)phenylenediamine) ligands and their derivatives are gaining increasing popularity because of their unique catalytic activities on broad range of chemical transformations [30-35], their use as building blocks in supramolecular chemistry [36,37], and in materials chemistry [38]. Moreover, salen/salophen-zinc(II) complexes are additionally most challenging issue since the above mentioned biological relevancy of the metal [39-43]. In association with this subject, salen/salophen-zinc(II) complexes are known to be efficient fluorescence emitters displaying long fluorescence life-time and high quantum yield, and hence, qualified as quite appealing candidates for use in contemporary biosensory applications for biologically relevant anions and molecules [44-47], in the design of OLED materials [48,49] and in fluorescence detection of nitro-based chemical explosives [50-52]. Numerous papers dealing with fluorescence applications of salen/salophen templated zinc(II) complexes have been appeared [25,26,52,44-47, 53-56] in most of which, complexation of non-emissive Schiff base ligand with zinc(II) resulted appreciably emissive square-planar structure to which, coordination of analytes also quenches the fluorescence mostly through Photo-induced electron transfer (PET) pathway. In the study reported herein, the salen template was modified by replacing salicylidamine and ethylenediamine moieties with 2-hydroxy naphthalidimine and 2,3-diaminopropane counterparts respectively. The complexation of obtained emissive Schiff base ligand napdap with zinc(II), exhibited additional visible-region fluorescence adding to the slight enhancement of ligand based one. The origins and characters of the excited states responsible for the fluorescences have been further investigated by quantum chemical TD-DFT calculations.

## EXPERIMENTAL

### Materials and Measurements

All reagents and solvents were purchased from commercial suppliers and used as received unless specified. Elemental analyses were performed on a LECO CHNS-932 analyzer (USA). IR spectra were recorded on a Bruker Vertex-80V ATR/FT-IR spectrometer (GERMANY) in the region 4000-400  $\text{cm}^{-1}$  sampling as KBr pellets. UV-Vis spectra were recorded on a Unicam UV2 UV-Vis spectrometer (USA) within 200-800 nm range, in THF medium. ESI-MS spectra were recorded in methanol on an AB SCIEX QTRAP® 5500 LC/MS/MS SYSTEM Mass spectrometer (USA): The samples were dissolved in hypergrade methanol stirring in a Banderin Sonorex ultrasonic bath and infusion (continuous signal) method with a flow rate of 5-20  $\mu\text{m}/\text{min}$  was used for mass scanning. Fluorescence spectra were recorded in 320-600 nm range on a QuantaMasterTM 30 steady state spectrofluorometer (ENGLAND). Conductivity measurement were performed with a HACH HQ40d portable multi-paramter meter using 10-4 M THF-acetonitril (2:1) solution. Thermal analysis measurements were conducted in statical air atmosphere by using a Shimadzu Thermal Analyzer equipment with a DTG-60 detector (JAPAN) in 10°C/sec. heating rate, within 20-1000°C range and using 3-8 mg samples.

Fluorescence quantum yields ( $\phi$ ) of napdap and 1 were estimated for their THF solutions by a relative method using anthracene as reference standard (ex=320 nm,  $\phi=0.27$  in ethanol) [57]. The quantum yields of samples were calculated using

$$\phi = \phi_R \frac{I}{I_R} \frac{OD_R}{OD} \frac{n^2}{n_R^2}$$

Where I is integrated fluorescence intensity, OD is the optical density (absorbance) at the wavelength of exciting light, and n is the refractive index of the medium [58]. The absorbance values for the calculation of quantum yields were purposely chosen under 0.1 to eliminate inner filter effects.

### Synthesis of N,N -bis(2-hydroxy-naphthaldimine)-propane (napdap)

2-hydroxynaphthaldehyde (0.690 g, 4 mmol) was dissolved in absolute ethanol and to this solution, an ethanolic solution of 2,3-diaminopropane (0.150 g, 2 mmol) was added and the mixture was refluxed for 2 hours at 50°C. The resulting bright yellow precipitate of the Schiff base was filtered, washed with cold ethanol and dried in air. Yield: 92%. Anal. calc. C = 75.00%; H = 6.00%; N = 7.00%. Found C = 76.58%; H = 5.98%; N = 7.13%. IR (KBr,  $\text{cm}^{-1}$ ): 2955 as(C-H); 3027 as(C-Harom); 1627 (C=N); 1207 (C-Ophenol). ESI-MS (m/z): 382 (napdap+, %100)

### Synthesis of 1

To the above prepared napdap ( $\approx 2$  mmol, 0.780 g) dissolved in THF, a solution of  $\text{ZnClO}_4 \cdot 6\text{H}_2\text{O}$  (2 mmol, 0.770 g) in THF was added dropwise. After a short while, resulting pale yellow precipitate of 1 was filtered, washed with cold THF, and analyzed. Yield: 62%. Anal. Calc. C = 64.51%; H = 4.73%; N = 6.02%. Found C = 62.23%; H = 4.97%; N = 5.84%. IR (KBr,  $\text{cm}^{-1}$ ): 2921 as(C-H); 3048 as(C-Harom); 1606 (C=N); 1359 (C-Ophenol). ESI-MS (m/z): 447 ( $\text{H}_2^{12+}$ , 100%), 110 (91.48%), 102 (10.24%). Thermal analysis (TGA): (total weight loss calc. = 81.88%, found = 82.54% relative to the mass of calculated final product ZnO) (see thermal analysis plots of 1 in Figure 1 in Supplementary data).

### Computational Details

All calculations were performed using GAUSSIAN 09 suit of programs running under Windows [59]. First input geometries of napdap and 1 for the initial gas-phase geometry optimizations were arbitrarily generated utilizing from experimental data, and all subsequent calculations were performed based on optimized geometries. B3LYP hybrid functional along with flexible double zeta LANL2DZ basis set with ECP was used for all calculations. Solvent media optimizations were performed by simulating the medium with PCM solvation model [60,61]. PCM/TD-DFT calculation was performed for the first singlet 70 vertical excitations. The calculated transitions were assumed to take place between ground state Kohn-Sham molecular orbitals (MO) to predict the

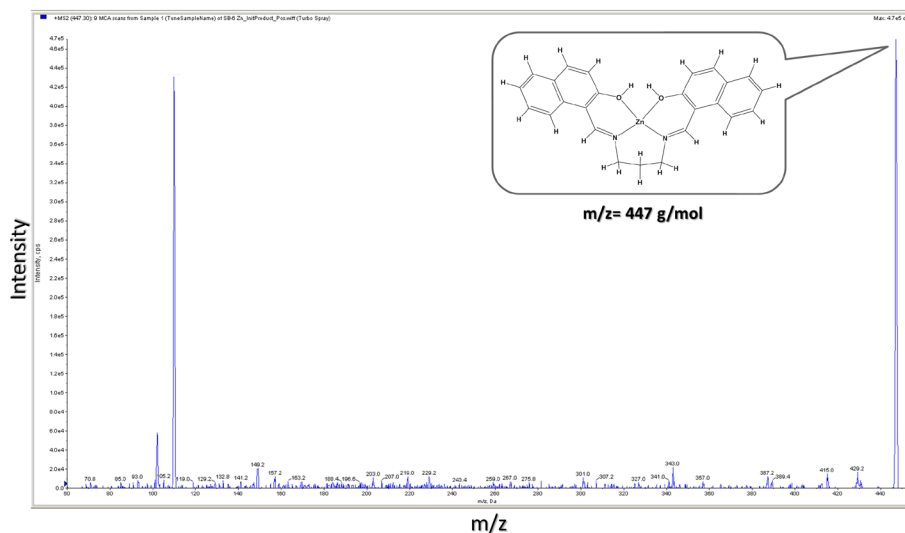


**Figure 1.** ESI-mass spectrum of 1 monitored m/z=60-450 range.

assignments and characters of the experimental transitions. Molecular orbital contributions (MOC) were computed by using GausSum 2.2.5 software [62]. Simulation of calculated spectra were made by using SWIZARD program [63,64].

## RESULTS AND DISCUSSION

### ESI-Mass Spectroscopy

In addition to the matching of IR, Elemental analysis and conductivity measurements data for the proposed structure of 1, ESI-Mass spectroscopic data shows more obviously the formation of 1 with the most abundant peak at m/z = 447 g/mol in mass spectrum of 1 in Figure 1 (see the chromatogram and mass spectrum of napdap in Figure 2 in Supplementary data). The peak at m/z = 447 g/mol is related to the protonated form of 1 ( $H_2^{12+}$ ) in solution, Since ESI-mass spectra were recorded in positive ion mode and in this mode, charging of the sample occurs preferably by proton transfer to the complex (keeping the spraying nozzle at positive potential) [65]. Furthermore, molar conductance data ( $\Lambda = 100 \text{ s}\cdot\text{cm}^2/\text{mol}$ ), the entire absences of perchlorate signals related to IR and mass spectra, thermal analysis and elemental analyses data clearly verify the neutral deprotonated form of 1 (see IR spectra of napdap and 1 in Figure 3 and S4 respectively in supplementary data). The peak at m/z = 110 g/mol is related to unassigned partial fragmentation product of 1. The strongest peak corresponding to  $H_2^{12+}$  indicates that 1 remains

intact towards fragmentation during ionization process.

### Ground State Structures of Compounds

Gas-phase optimized geometry of napdap with Cs symmetry and that of 1 with C<sub>2v</sub> symmetry are given in Figure 2. MOC from central ion, naphthalene rings, azomethine moities oxygen donors in 1 and hydroxyl groups in napdap are given in Table 1. The values in the table are the sum of symmetry related moities of the complex. As inferred from the table, almost non of contribution from zinc (II) to the frontier molecular orbitals (FMOs) is calculated. HOMO<sup>-1</sup> with HOMO-2 and LUMO+2 with LUMO+3 are identical among each other with the same energy and the same amount of contributions from the groups. It is also noteworthy that the large contributions to the LUMO and LUMO+2 from small azomethine groups and no contribution from propylene moiety to all FMOS are involved (see convoluted spectrum of 1 indicating relative contributions of the groups of interest in Figure 5 in Supplementary data). In free ligand, both low lying virtual and occupied molecular orbitals (HOMO-HOMO<sup>-1</sup> and LUMO-LUMO+1) are additionally degenerated among each other as seen in Table 1. As compared in Figure 3, FMOs in 1 are more delocalized than these in napdap as a result of coordination to zinc (II) ion despite both compounds are in planar conformation.

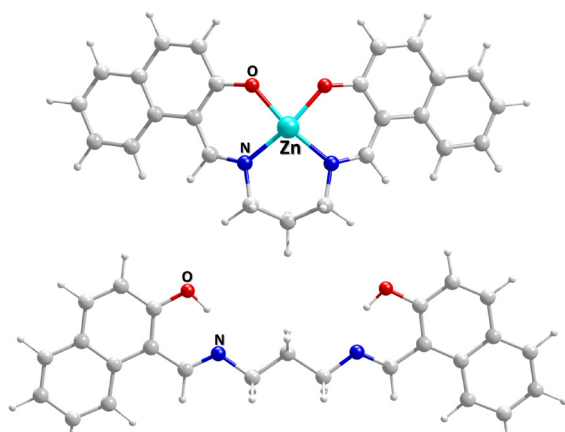


**Figure 2.** Optimized geometries of napdap (bottom) and 1 (top).

**Table 1.** MOC of selected MOs from molecular moieties in napdap and 1.

MO	H		H <sup>1</sup>		H-2		H-3		L		L+1		L+2	
Molecule	napdap	1	napdap	1	napdap	1	napdap	1	napdap	1	napdap	1	napdap	1
E (eV)	-5.85	-5.37	-5.87	-5.57	-6.53	-6.19	-6.53	-6.21	-1.88	-1.80	-1.87	-1.68	-0.77	-0.68
Moiety														
Zn	-	0	-	3	-	0	-	0	-	0	-	0	-	3
Naph	76	64	78	68	90	92	90	92	58	48	58	54	70	78
Azomet.	12	14	12	14	0	2	0	2	38	44	38	40	30	18
Propyl.	0	0	0	0	0	0	0	0	0	1	0	0	0	0
Oxy.	-	20	-	16	-	6	-	6	-	8	-	6	-	0
Hydrox.	10	-	10	-	8	-	8	-	4	-	4	-	0	-

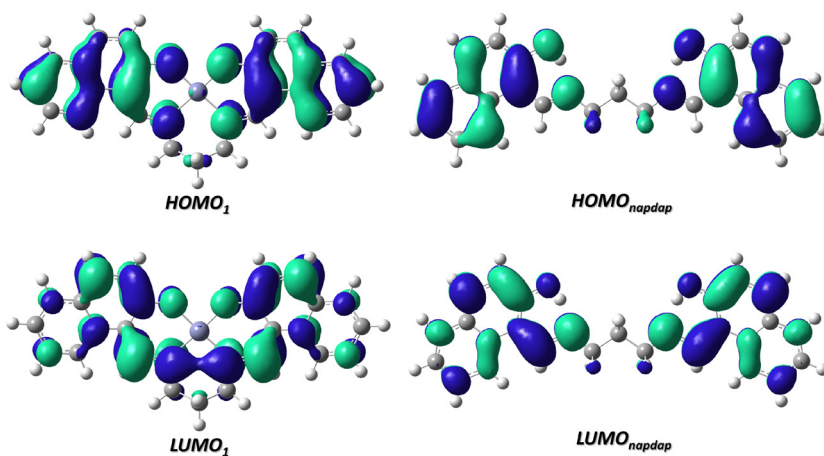


**Figure 3.** FMOs of napdap and 1 with 0.02 isovalues.

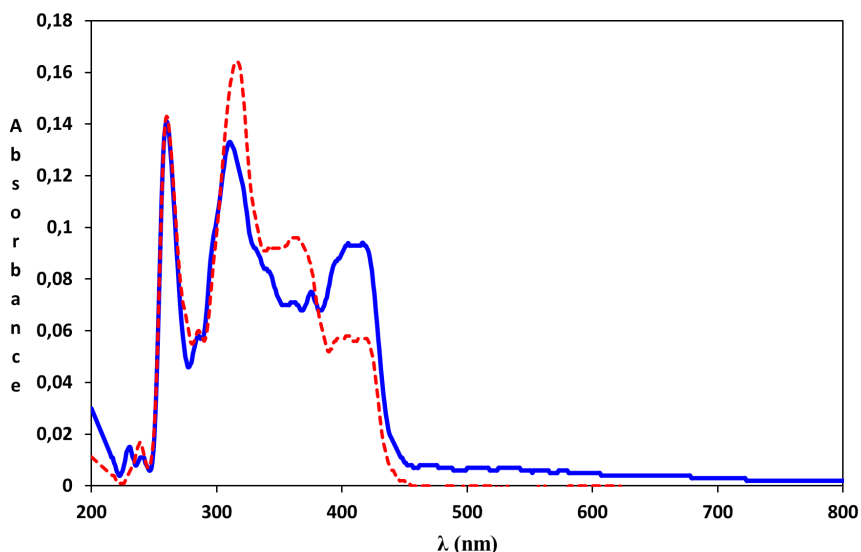


**Figure 4.** Overlaid absorption profiles of napdap (solid line) and 1 (dashed line).

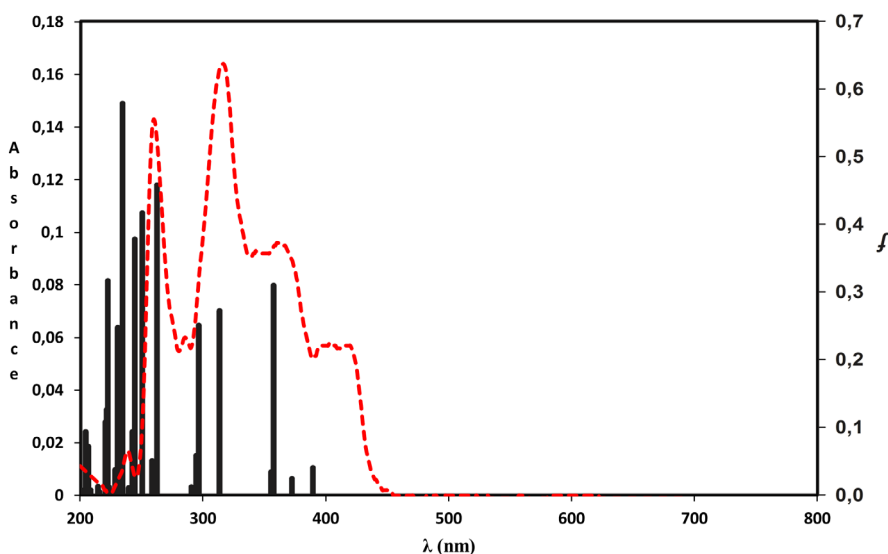


**Figure 5.** Calculated (oscillator strengths) and experimental (curve) spectra of 1.

### Excited States, Emission Spectra and TD-DFT Calculation

An overlays of absorption profiles of napdap and 1 is shown in Figure 4. Upon complexation with zinc(II), not a strict changes in energy were observed though accompanying increment in absorbances as can be seen from Figure 4. This result indicates that the naphthalene and azomethine  $\pi \rightarrow \pi^*$  transitions of napdap are in principle metal-independent.

In the superimposed calculated and experimental spectra of 1 in Figure 5, most of the transitions of larger oscillator strengths are populated in the middle-UV region of the spectrum and are completely naphthalene-centered transitions in character. Tables 2 and 3 show the excitation parameters of important calculated and experimental transitions in napdap and 1 respectively.

**Table 2.** Important excited state parameters of 1.

State	Transition	(nm)		<i>f</i>	$\Delta E$ (eV)	o $\rightarrow$ v(%Cont.)	Character/ Assignment
		Expl.	Calc.				
3 <sup>1</sup> A'	<sup>1</sup> A' $\rightarrow$ <sup>1</sup> A'*	362	357	0.3096	3.47	H <sup>1</sup> $\rightarrow$ L(65%)	ILCT/(naph- $\pi$ $\rightarrow$ naph/ azomet.- $\pi$ *)
						H $\rightarrow$ L+2(16%)	
7 <sup>1</sup> A''	<sup>1</sup> A'' $\rightarrow$ <sup>1</sup> A''*	317	313	0.2723	3.96	H-2 $\rightarrow$ L(63%)	ILCT/(naph- $\pi$ $\rightarrow$ naph/ azomet.- $\pi$ *)
						H-3 $\rightarrow$ L+1(22%)	
17 <sup>1</sup> A''	<sup>1</sup> A' $\rightarrow$ <sup>1</sup> A''*	260	262	0.4581	4.73	H $\rightarrow$ L+4(51%)	ILCT/(naph- $\pi$ $\rightarrow$ naph- $\pi$ *)
19 <sup>1</sup> A''	<sup>1</sup> A' $\rightarrow$ <sup>1</sup> A''*	-	250	0.4167	4.97	H $\rightarrow$ L+4(32%)	ILCT/(naph- $\pi$ $\rightarrow$ naph- $\pi$ *)
						H-6 $\rightarrow$ L(21%)	ILCT/(naph- $\pi$ $\rightarrow$ naph/ azomet.- $\pi$ *)
21 <sup>1</sup> A''	<sup>1</sup> A' $\rightarrow$ <sup>1</sup> A''*	237	244	0.3780	5.09	H <sup>1</sup> $\rightarrow$ L+5(44%)	ILCT/(naph- $\pi$ $\rightarrow$ naph- $\pi$ *)
						H-6 $\rightarrow$ L(34%)	
25 <sup>1</sup> A''	<sup>1</sup> A' $\rightarrow$ <sup>1</sup> A''*	-	234	0.5788	5.31	H-2 $\rightarrow$ L+2(46%)	ILCT/(naph- $\pi$ $\rightarrow$ naph- $\pi$ *)

**Table 3.** Important excited state parameters of napdap.

State	Transition	(nm)		<i>f</i>	$\Delta E$ (eV)	o $\rightarrow$ v(%Cont.)	Character/ Assignment
		Expl.	Calc.				
1 <sup>1</sup> A1	<sup>1</sup> A2 $\rightarrow$ <sup>1</sup> B1*	378	342	0.3913	3.62	H $\rightarrow$ L(61%)	ILCT/(naph- $\pi$ $\rightarrow$ naph/ azomet.- $\pi$ *)
						H <sup>1</sup> $\rightarrow$ L+1(22%)	
2 <sup>1</sup> A1	<sup>1</sup> A1 $\rightarrow$ <sup>1</sup> B1*	-	337	0.1291	3.67	H <sup>1</sup> $\rightarrow$ L(43%)	ILCT/(naph- $\pi$ $\rightarrow$ naph/ azomet.- $\pi$ *)
						H $\rightarrow$ L+1(38%)	
5 <sup>1</sup> B2	<sup>1</sup> A2 $\rightarrow$ <sup>1</sup> B1*	310	304	0.1820	4.07	H-3 $\rightarrow$ L(41%)	ILCT/(naph- $\pi$ $\rightarrow$ naph/ azomet.- $\pi$ *)
						H-2 $\rightarrow$ L+1(36%)	
14 <sup>1</sup> A1	<sup>1</sup> B1 $\rightarrow$ <sup>1</sup> B1*	260	253	0.1459	4.91	H-3 $\rightarrow$ L+2(17%)	ILCT/(naph- $\pi$ $\rightarrow$ naph- $\pi$ *)
						H-2 $\rightarrow$ L+3(16%)	ILCT/(naph- $\pi$ $\rightarrow$ naph- $\pi$ *)
19 <sup>1</sup> B2	<sup>1</sup> A2 $\rightarrow$ <sup>1</sup> B1*	-	239	1.0312	5.20	H-6 $\rightarrow$ L(43%)	ILCT/(naph/ azomet.- $\pi$ $\rightarrow$ naph/ azomet.- $\pi$ *)
						H-7 $\rightarrow$ L+1(24%)	
25 <sup>1</sup> B2	<sup>1</sup> A2 $\rightarrow$ <sup>1</sup> B1*	-	222	0.8091	5.57	H-2 $\rightarrow$ L+2(23%)	ILCT/(naph- $\pi$ $\rightarrow$ naph- $\pi$ *)
						H-3 $\rightarrow$ L+3(19%)	

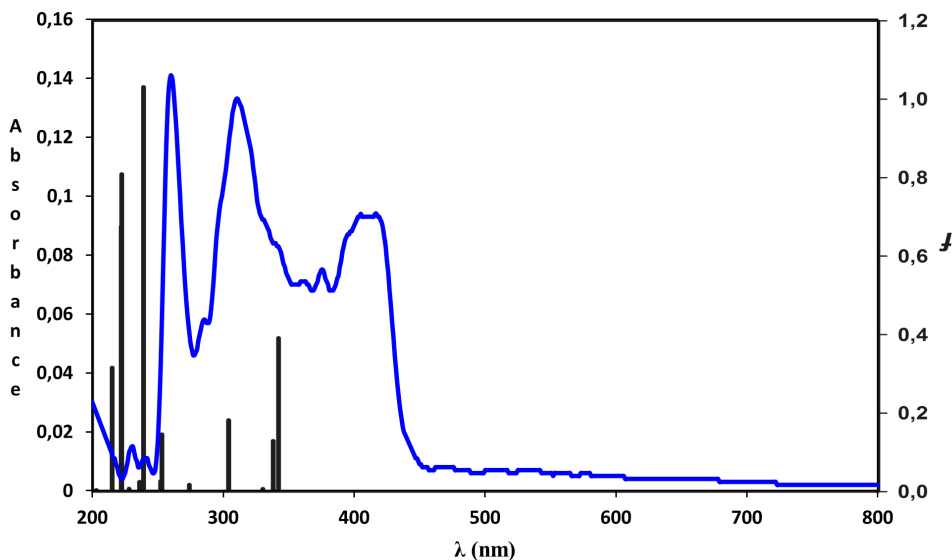


**Figure 6.** Calculated (oscillator strengths) and experimental (curve) spectra of napdap

Most of the observed transitions fairly coincide with the calculated ones in far-UV region of the spectrum in 1 and are successfully assigned while in case of napdap, the observed and calculated transitions are incompatible as seen in Table 3 and in superimposed spectra of napdap in Figure 6. Thus, assignments of the observed transitions were made by utilizing from that of 1. All transitions both in napdap and 1 designated with an Intra-ligand charge transfer (ILCT) configuration and as expected, none of transitions originating from metal-centered, metal-to-ligand or ligand-to-metal, charge transfer states in 1 were observed since Zn(II) ion is resistant to oxidation or reduction with its stable d10 electronic configuration. The designations of the observed transitions in Tables 2 and 3 were made by considering the transitions with the highest contributions.

The smoothed emission spectra of napdap and 1 together with steady-state excitation maximum is given in Figure 7 (see original spectra in Figure 6 in Supplementary data). On account of observed small Stokes shifts of napdap and 1, highly diluted solutions ( $10^{-6}$  M) were used for the fluorescence spectra to prevent from liable concentration quenching. Upon excitation at 316 nm, two distinct emission maxima at 356 nm and 443 nm were observed in 1 while only one peak in napdap was observed at the same wavelength with that of 1. This clearly shows that incorporation

of zinc(II) into the free ligand generates additional free ligand-independent 443 nm fluorescence and, the higher energy fluorescence is strictly inassociated with metal ion. It is clear that the more the delocalization throughout the molecule with strong planarity gained by the complexation and the higher the absorption and emissive responses. On the other hand, the low quantum yield of napdap ( $\phi_{\text{napdap}} = 0.0049$ ) is improved much less than expected by the incorporation of Zn(II) ( $\phi_1 = 0.0091$ ). This is most likely due to unforeseeable excimer formation which gives rise to lowering quantum efficiency of molecule. Since the lower energy and broader 443 nm emission most probably originates from excimer species.

In association with the fluorescence emissions, the absorption maxima at 310 and 317 nm in the spectra of napdap and 1 respectively consist mainly of two components as seen in Tables 2 and 3. In napdap, 51B2 state to which 310 nm excitation was assigned is mainly composed of almost equal contributions from HOMO-3→LUMO (41%) and HOMO-2→LUMO+1 (36%) transitions. These transitions take place between completely degenerated MOs (see Table 1) and thus, 51B2 state is in principle a doubly degenerated excited state ( $\Delta E_{\text{HOMO-3-HOMO-2}} = 0.00$  eV,  $\Delta E_{\text{LUMO-LUMO+1}} = 0.01$  eV for napdap). In case of 1, 317 nm excitation is assigned to 71A'' state and comprise

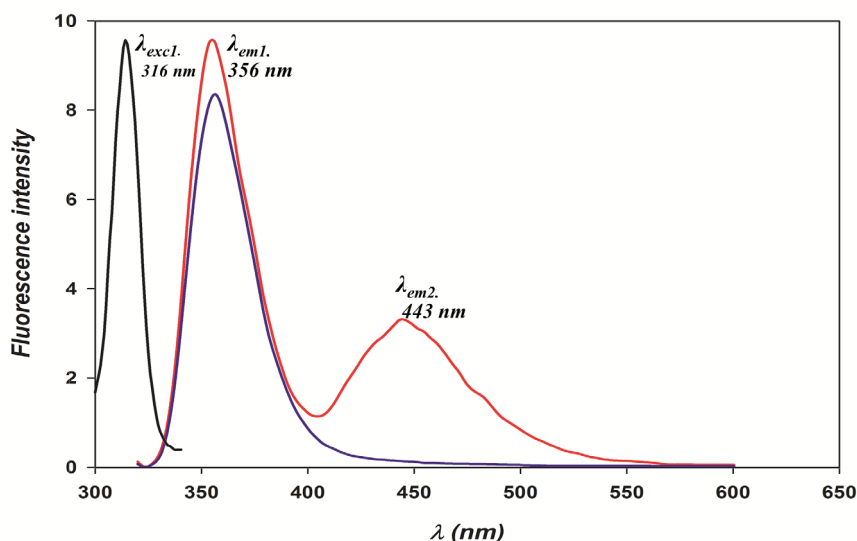


**Figure 7.** Smoothed emission spectra of napdap (violet) and 1 (red).

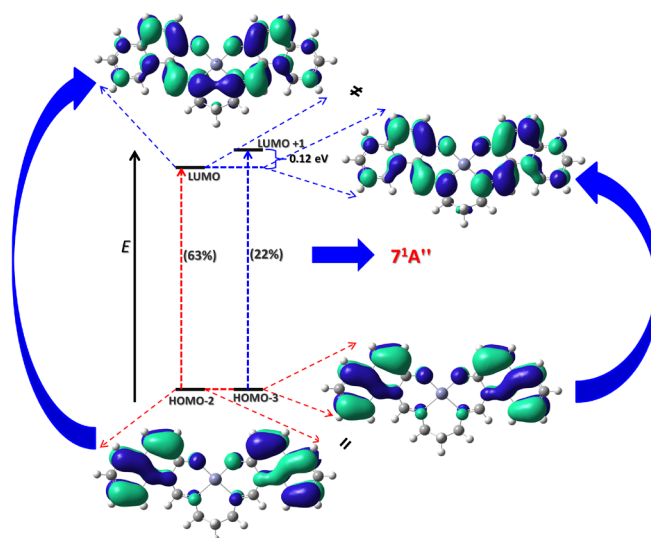


**Figure 8.** Schematized transitions of  $7^1A''$  state in 1 (= and  $\neq$  remarks denote near to degeneracy and non-degeneracy of MOs respectively).

much larger contribution from HOMO-2 $\rightarrow$ LUMO transition (63%) and in transition from napdap to 1, the degeneracy in this state is disappeared to some extent ( $\Delta E_{\text{HOMO-3-HOMO-2}} = 0.02$  eV,  $\Delta E_{\text{LUMO-LUMO+1}} = 0.12$  eV for 1). Based upon this change, one may say that  $7^1A''$  state in 1 is a two-component non-degenerate excited state in contrary to that in napdap as demonstrated in Figure 8. As a result, It is thought that the lower intensity 443 nm excimer emission in 1 is related to the radiative decay of the additional ILCT manifolds of the excited  $7^1A''$  state that are otherwise absent owing to degeneracy in case of napdap.

## CONCLUSIONS

Using 2-hydroxynaphthaldehyde and 1,3-diaminopropane precursors, a salen templated NNOO tetradentate Schiff base and corresponding zinc(II) complex have been prepared and characterized by elemental analyses, ESI-mass spectroscopy, FT-IR and conductivity measurements. Excitation and emission properties of the compounds have been studied by UV-Vis absorption and steady state fluorescence spectroscopy techniques. Emission measurements have shown that free ligand

napdap fluoresces with a maximum at 346 nm and its complexation with zinc(II) strengthened 346 nm ligand-based emission produced a new 443 nm fluorescence which is strictly associated with unexpected excimer formation though the emission measurements were made by using polar solvent. This unfavourable phenomenon probably is reinforced by large planar naphthalidimine moieties. Following a theoretical overview, TD-DFT calculations have suggested that the origin of this low intensity excimer fluorescence comes from ILCT transitions of non-degenerate 71A'' state.

As apart from the main scope of this study, it is possible and more rational that a significant improvement of the fluorescence quantum yields by making further explorations such as substitutions with proper bulky and solubility-increasing groups which lead to increasing and removal of excimer formation.

#### ACKNOWLEDGEMENTS

Assoc. Prof. Demet KAYA from İTÜ (İstanbul Technical University) for the fluorescence measurements is acknowledged. Forensic chemist Özgür TURNA from Trabzon Forensic Medicine Institution Trabzon/TURKEY for ESI-Mass spectroscopy measurements is also acknowledged.

---

#### References

---

- J.M. Bergi, Y. Shi, *Science*, 271 (1996) 1081.
- W.N. Lipscomb and N. Sträter, *Chem. Rev.*, 96 (1996) 2375-2433.
- J.J.R. Fausto da Silva, R.J.P. Williams, *The Biological Chemistry of the Elements: Oxford University Press, New York*, 1992.
- G. Jaouen, *Bioorganometallics: Biomolecules, Labeling, Medicine, Wiley-VCH, Paris*, 2005.
- J.P. Mackay, D.J. Segal, *Engineered Zinc Finger Proteins: Methods and Protocols, Springer, New York Heidelberg Dordrecht London*, 2010.
- P.D. Boyer, *The Enzymes: Hydrolysis: Peptide Bonds, Academic Press, New York and London*, 1971.
- H. Chen, Y. Wu, Y. Cheng, H. Yang, F. Li, P. Yang, C. Huang, *Inorg. Chem. Commun.* 10 (2207) 1413-1415.
- G.K. Andrews, *Biometals*, 14 (2001) 223-237.
- E.L. Que, D.W. Domaille and C.J. Chang, *Chem. Rev.*, 108 (2008) 1517-1549.
- B.L. Vallee and K.H. Falchuk, *Physiol. Rev.*, 73 (1993) 79-118.
- C.J. Frederickson, J.Y. Koh, A.I. Bush, *Nat. Rev. Neurosci.*, 6 (2005) 449-462.
- L.C. Costello, R.B. Franklin *Mol. Cancer*, 5 (2206) 59-63.
- M. Mager, W.F. McNary, F.J. Lionetti, *Histochem. Cytochem.*, 1 (1953) 493-504.
- C.G. Taylor, *Biometals*, 18 (2005) 305-312.
- P.D. Zalewski, X. Jian, L.L.L. Soon, W.G. Breed, R.F. Seamark, S.F. Lincoln, A.D. Ward, F.Z. Sun, *Reprod. Fertil. Dev.*, 8 (1996) 1097-1105.
- A.I. Bush, W.H. Pettingell, G. Multhaup, M.D. Paradis, J.P. Vonsattel, J.F. Gusella, K. Beyreuther, C.L. Masters, R.E. Tanzi, *Science*, 265 (1994) 1464-1467.
- A.Q. Truong-Tran, L.H. Ho, F. Chai, P.D. Zalewski, *J. Nutr.*, 130 (2000) 1459S-1466.
- C.J. Frederickson, M.D. Hernandez, J.F. McGinty, *Brain Res.*, 480 (1989) 317-321.
- M.P. Cuajungco, G.J. Less, *Neurobiol. Dis.*, 4 (1997) 137-169.
- D.W. Choi, J.Y. Koh, *Annu. Rev. Neurosci.*, 21 (1998) 347-375.
- J.H. Weiss, S.L. Sensi, J.K. Koh, *Trends Pharmacol. Sci.*, 21 (2000) 395-401.
- S.W. Suh, K.B. Jensen, M.S. Jensen, D.S. Silva, P.J. Kessler, G. Danscher, C.J. Frederickson, *Brain Res.*, 852 (2000) 274-278.
- A.I. Bush, *Alzheimer Dis. Assoc. Disord.*, 17 (2003) 147-150.
- M.S. Wold, *Annu. Rev. Biochem.*, 66 (1997) 61-62.
- S. Majumder, L. Mandal, S. Mohanta, *Inorg. Chem.*, 51 (2012) 8739-8749.
- K. Hanaoka, K. Kikuchi, H. Kojima, Y. Urano, and T. Nagano, *J. Am. Chem. Soc.*, 126 (2004) 12470-12476.
- K. Kikuchi, K. Komatsu, T. Nagano, *Curr. Opin. Chem. Biol.*, 8 (2004) 182-191.
- P. Jiang, Z. Guo, *Coord. Chem. Rev.*, 248 (2004) 205-229.
- S.C. Burdette and S.J. Lippard, *Inorg. Chem.*, 41 (2002) 6816-6823.
- E.N. Jacobsen, in *Comprehensive Organometallic Chemistry II* (Eds. E.W. Abel, F.G.A. Stone, and E. Willinson, Pergamon, New York, 12 (1995) 1097-1135.
- T.M. Oviatt, G.W. Coates, *J. Am. Chem. Soc.* 121 (1999) 4072-4073.
- D.A. Atwood, M.J. Harvey, *J. Chem. Rev.*, 101 (2001) 37-52.
- C.T. Cohen, T. Chu, G.W. Coates, *J. Am. Chem. Soc.*, 127 (2005) 10869-10878.
- L. Canali, D.C. Sherrington, *Chem. Soc. Rev.*, 28 (1999) 85-93.
- R.G. Konsler, J. Karl, E.N. Jacobsen, *J. Am. Chem. Soc.*, 120 (1998) 10780-10781.
- A.W. Kleij, M. Kuil, M. Lutz, D.M. Tooke, A.L. Spek, P.C.J. Kamer, P.W.N.M. van Leeuwen, J.N.H. Reek, *Inorg. Chim. Acta*, 359 (2006) 1807-1814.
- A.W. Kleij, M. Kuil, D.M. Tooke, A.L. Spek, J.N.H. Reek, *Chem.-Eur. J.*, 11 (2005) 4743-4750.
- P.G. Lacroix, *Eur. J. Inorg. Chem.*, (2001) 339-348.
- R. Brissos, D. Ramos, J.C. Lima, F.Y. Mihan, M. Borràs, J. De Lapuente, A. Dalla Cort and L. Rodríguez, *New J. Chem.* (2013) DOI: 10.1039/c3nj41125g
- S.I. Pasco, P.A. Waghorn, T.D. Conry, B. Lin, H.M. Betts, J.R. Dilworth, R.B. Sim, G.C. Churcill, F.I. Aigbirhio, and J.E. Warren, *Dalton Trans.*, (2008) 2107-2110.
- G. Consiglio, S. Failla, P. Finocchiaro, I.P. Oliveri and S. Di Bella, *Dalton Trans.*, 47 (2012) 387-395.
- A.L. Singer and D.A. Atwood, *Inorg. Chim. Acta*, 277 (1998) 157-162.

43. Y. Gao, J. Wu, Y. Li, P. Sun, H. Zhou, J. Yang, S. Zhang, B. Jin and Y. Tian, *J. Am. Chem. Soc.*, 131 (2009) 5208-5213.
44. M. Cano, L. Rodríguez, J.C. Lima, F. Pina, A. Dalla Cort, C. Pasquini, and L. Schiaffino, *Inorg. Chem.*, 48 (2009) 6229-6235.
45. I.P. Oliveri and S. Di Bella, *J. Phys. Chem.*, A 115 (2011) 14325-14330.
46. E.C. Escudero-Adán, J. Benet-Buchholz, and A.W. Kleij, *Inorg. Chem.*, 47 (2008) 4256-4263.
47. S. Khatua, S.H. Choi, J. Lee, K. Kim, Y. Do, and D.G. Churchill, *Inorg. Chem.*, 48 (2009) 2993-2999.
48. Y. Hamada, T. Sano, M. Fujita, T. Fujii, Y. Nishio, K. Shibata, *Jpn. J. Appl. Phys.*, 32 (1993) L511-L513.
49. T. Sano, Y. Nishio, Y. Hamada, H. Takahashi, T. Usuki, K. Shibata, *K. J. Mater. Chem.*, 10 (2000) 157-161.
50. M.E. Germain, T.R. Vargo, B.A. McClure, J.J. Rack, P.G. Van Petten, M. Odoi, and M.J. Knapp, *Inorg. Chem.*, 47 (2008) 6203-6211
51. M.E. Germain and M.J. Knapp, *J. Am. Chem. Soc.*, 130 (2008) 5422-5423.
52. M.E. Germain, T.R. Vargo, P.G. Khalifah, and M.J. Knapp, *Inorg. Chem.*, 46 (2007) 4422-4429.
53. K.-H Chang, C.-C. Huang, Y.-H. Liu, Y.-H. Hu, P.-T. Chou and Y.-C. Lin, *Dalton Trans.*, (2004) 1731-1738.
54. S. Di Bella, N. Leonardi, G. Consiglio, S. Sortino, and I. Fragalà, *Eur. J. Inorg. Chem.*, (2004) 4561-1565.
55. G. Consiglio, S. Failla, I.P. Oliveri, R. Purrello and S. Di Bella, *Dalton Trans.*, (2009) 10426-10428.
56. Q. Meng, P. Zhou, F. Song, Y. Wang, G. Liu and H. Li, *Cryst. Eng. Comm.*, 15 (2013) 2786-2790.
57. W.R. Dawson and M.W. Windsor, *J. Phys. Chem.*, 72 (1968) 3251-3260.
58. J.R. Lakowicz, *Principles of Fluorescence Spectroscopy*: Springer, University of Maryland School of Medicine, Baltimore, Maryland, 2006.
59. Gaussian 09, Revision A.1, M.J. Frisch, G.W. Trucks, H.B. Schlegel, G. E. Scuseria, M. A. Robb, J. R. Cheeseman, G. Scalmani, V. Barone, B. Mennucci, G.A. Petersson, H. Nakatsuji, M. Caricato, X. Li, H.P. Hratchian, A. F. Izmaylov, J. Bloino, G. Zheng, J.L. Sonnenberg, M. Hada, M. Ehara, K. Toyota, R. Fukuda, J. Hasegawa, M. Ishida, T. Nakajima, Y. Honda, O. Kitao, H. Nakai, T. Vreven, J.A. Montgomery, Jr., J.E. Peralta, F. Ogliaro, M. Bearpark, J.J. Heyd, E. Brothers, K.N. Kudin, V.N. Staroverov, R. Kobayashi, J. Normand, K. Raghavachari, A. Rendell, J.C. Burant, S.S. Iyengar, J. Tomasi, M. Cossi, N. Rega, J.M. Millam, M. Klene, J.E. Knox, J.B. Cross, V. Bakken, C. Adamo, J. Jaramillo, R. Gomperts, R.E. Stratmann, O. Yazyev, A.J. Austin, R. Cammi, C. Pomelli, J.W. Ochterski, R.L. Martin, K. Morokuma, V.G. Zakrzewski, G.A. Voth, P. Salvador, J. J. Dannenberg, S. Dapprich, A.D. Daniels, Ö. Farkas, J. B. Foresman, J.V. Ortiz, J. Cioslowski, and D.J. Fox, Gaussian, Inc., Wallingford CT, 2009.
60. J. Tomasi, M. Persico, *Chem. Rev.*, (1994) 2027-2094.
61. J. Tomasi, B. Mennucci, and R. Cammi, *Chem. Rev.*, (2005) 2999-3093.
62. N.M. O'Boyle, A.L. Tenderholt and K.M. Langner, *J. Comp. Chem.*, 29 (2008) 839-845.
63. S.I. Gorelsky, SWIZARD program, University of Ottawa, Ottawa, Canada, <http://www.sg-chem.net/>, 2012.
64. S.I. Gorelsky, A.B.P. Lever, *J. Organomet. Chem.*, 635 (2001) 187.
65. J.F.J. Todd, *Pure Appl. Chem.*, 63 (1991) 1541-1566.

